

- Fait, J. (1991). *XSCANS Users Manual*. Siemens Analytical X-ray Instruments Inc., Madison, Wisconsin, USA.
- Kamenar, B. (1963). *Acta Cryst.* **16**, A-34.
- Sheldrick, G. M. (1990). *SHELXTL/PC Users Manual*. Siemens Analytical X-ray Instruments Inc., Madison, Wisconsin, USA.
- Sheldrick, G. M. (1995). *SHELXTL/PC*. Version 5.03. Siemens Analytical X-ray Instruments Inc., Madison, Wisconsin, USA.
- Sheldrick, G. M. & Taylor, R. (1975). *Acta Cryst.* **B31**, 2740–2741.

Acta Cryst. (1997). **C53**, 1602–1605

Steric Hindrance in a Mixed Solvated Nickel(II) Complex: Bis(acetonitrile-*N*)-tetrakis(*N,N*-dimethylacetamide-*O*)-nickel(II) Bis(tetrafluoroborate)

HONOH SUZUKI AND SHIN-ICHI ISHIGURO

Department of Chemistry, Kyushu University, 6-10-1
Hakozaki Higashi-ku, Fukuoka 812-81, Japan. E-mail:
suzukscc@mbox.nc.kyushu-u.ac.jp

(Received 6 March 1997; accepted 26 June 1997)

Abstract

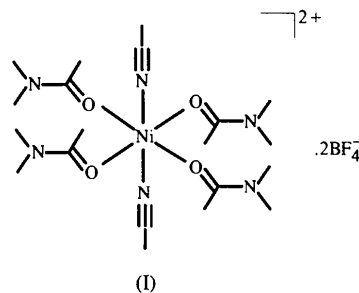
The title compound, [Ni(CH₃CN)₂{(CH₃)₂NCOCH₃}₄](BF₄)₂, has an octahedral coordination structure with the centre of symmetry at the Ni atom. Both of the two crystallographically inequivalent *N,N*-dimethylacetamide (DMA) molecules have normal coordination Ni—O bond lengths and Ni—O—C angles, but one of the Ni—O—C—N torsion angles deviates from 180°, indicating that the Ni—O bond is displaced from the direction of the lone pair of the *sp*²-O atom. This is ascribed to the steric hindrance of DMA coordination in an octahedral environment, which is imposed by the non-bonding contact of the acetyl methyl group with the ligating O atom of the adjacent DMA molecule.

Comment

Our thermodynamic studies of complexation equilibria in DMA solution have revealed activation of the solvated metal ions (Suzuki & Ishiguro, 1992). Unusual coordination structures such as five-coordinate [NiCl(DMA)₄]⁺ are also found in DMA. Because this solvent effect is encountered in various metal–ligand systems but never observed in an analogous solvent *N,N*-dimethylformamide (DMF), we have ascribed it to the steric hindrance of the acetyl methyl group of DMA, which may destabilize the solvation structure and cause the less-crowded complexes to emerge in solution. The difference between DMA and DMF disappears in the

case of tetrahedral complexes, which also supports the idea (Koide, Suzuki & Ishiguro, 1995).

An EXAFS study in DMF and DMA solutions, however, showed no difference in the solvation structures of bivalent transition metal ions except for Zn²⁺; all the ions but Zn²⁺ have an octahedral coordination structure [M^{II}(solvent)₆]²⁺ (*M* = Mn, Co, Ni, Cu) and the *M*—O bond lengths are almost identical in the two solvents (Ozutsumi, Koide, Suzuki & Ishiguro, 1993). To clarify detailed structural features of the steric hindrance in DMA coordination, we have isolated a hygroscopic crystal of the title compound, (I), from a mixture of acetonitrile and diethyl ether, and performed an X-ray diffraction analysis on the single crystal.



The structure (Fig. 1) shows that the Ni²⁺ ion has a centrosymmetric octahedral coordination environment in which both acetonitrile and DMA coordinate. Both of the crystallographically inequivalent DMA molecules have normal bond lengths (Ni—O) and angles (Ni—O—C) (Herceg & Fischer, 1974; Lemoine & Herpin, 1980; Ozutsumi *et al.*, 1993). Nevertheless, the Ni—O—C—N (τ) torsion angles in Table 2, which serve as a measure of coplanarity between the metal and the molecular plane of DMA, indicate that the coordinating conformation of the two DMA molecules is clearly distinguishable: ‘regular’ and ‘twisted’. One of the DMA molecules (O1—C14) is almost coplanar with Ni ($\tau = -170^\circ$), and the coordination occurs approximately in the direction of the lone pair of the *sp*²-O atom. The other (O2—C24), however, has $\tau = -113^\circ$; thus, the metal is largely out of the DMA molecular plane, *i.e.* the coordinated DMA is twisted around the O2—C21 bond.

Similar distortion is found in [Cu(DMA)₄(ClO₄)₂], where two of the DMA molecules have τ (Cu—O—C—N) = -165° and the other two have $\tau = 125^\circ$ (Lemoine & Herpin, 1980). On the other hand, all the τ (*M*—O—C—N) torsion angles are 172–176° in tetrahedral coordination structures [M^{II}Cl₂(DMA)₂] (*M* = Co, Zn) (Lindner, Perdikatsis & Thasitis, 1973; Herceg & Fischer, 1974). In DMF solvates, the torsion angles are 161–179° both in octahedral (Baumgartner, 1986; Young, Walters & Dewan, 1989) and tetrahedral structures (Suzuki, Fukushima, Ishiguro, Masuda & Ohtaki, 1991). Accordingly, the acetyl methyl group of DMA

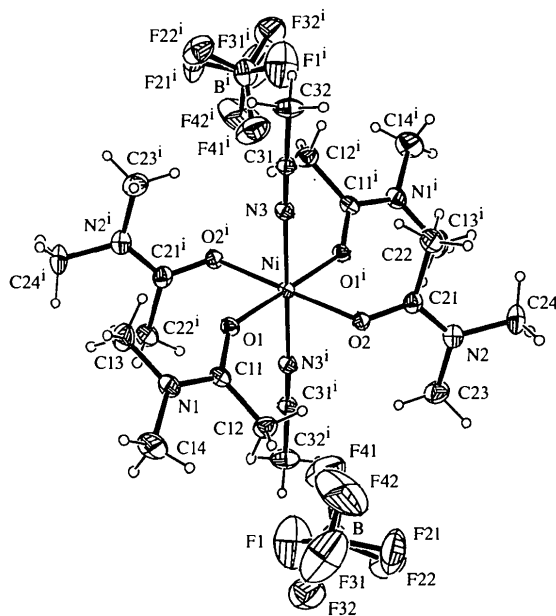


Fig. 1. Molecular diagram of $[\text{Ni}(\text{CH}_3\text{CN})_2\{(\text{CH}_3)_2\text{NCOCH}_3\}_4](\text{BF}_4)_2$ showing the labelling of the non-H atoms [symmetry operation: (i) $-x, -y, -z$]. Displacement ellipsoids are shown at 30% probability levels; H atoms are drawn as small circles of arbitrary radii.

must be responsible for the distortion that is specific to the octahedral environment.

The acetyl methyl C atoms (C12 and C22 in Fig. 2a) come close to adjacent ligating atoms in the octahedral coordination. The non-bonding distances are similar to or slightly shorter than the van der Waals closest approach (Bondi, 1964): $\text{C12}\cdots\text{O2} = 3.310$ (4), $\text{C12}\cdots\text{N3}^i = 3.322$ (5), $\text{C22}\cdots\text{O1}^i = 3.435$ (5) and $\text{C22}\cdots\text{N3} = 3.388$ (5) Å [symmetry operation: (i) $-x, -y, -z$].

In the structure, however, steric interactions responsible for the distortion are not readily seen because they are already relaxed. To see what causes the distortion, we examined a hypothetical 'regular' conformation for the 'twisted' DMA. Alternative positions, labelled as $\text{O2}^*-\text{C24}^*$ in Fig. 2(b), were generated by 90° rotation of the DMA moiety ($\text{O1}^i-\text{C14}^i$) around the Ni—N3 axis; this would correspond to the conformation in which all the DMA molecules were 'regular'. It results in shorter contact distances of $\text{C22}^*\cdots\text{O1}^i = 3.23$ and $\text{C22}^*\cdots\text{N3} = 3.32$ Å. The distance between two methyl C atoms $\text{C23}^*\cdots\text{C12} = 3.44$ Å is also close to the shortest contact distance (Bondi, 1964), which may be responsible for the twist to some extent. More importantly, because C22^* and the adjacent DMA ($\text{O1}^i-\text{C14}^i$) are on the same side of the Ni equatorial plane ($\text{O1}-\text{O2}^*-\text{O1}^i-\text{O2}^i$), C22^* approaches O1^i in the direction almost perpendicular to the molecular plane of $\text{O1}^i-\text{C14}^i$. Deviation from perpendicularity (the angle between the $\text{C22}^*\cdots\text{O1}^i$ vector and the normal vector to the plane)

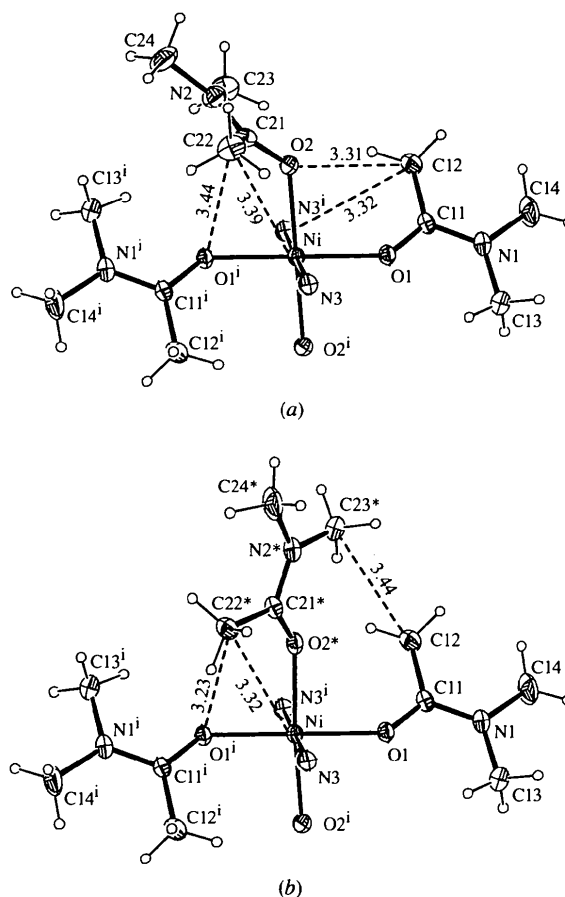


Fig. 2. Diagrams showing non-bonding contacts between three-coordinated DMA molecules. The other ligands have been omitted for clarity. (a) The 'twisted' DMA ($\text{O2}-\text{C24}$) and the adjacent 'regular' DMA molecules ($\text{O1}-\text{C14}$ and $\text{O1}^i-\text{C14}^i$). (b) A hypothetical 'regular' DMA ($\text{O2}^*-\text{C24}^*$) generated by 90° rotation of $\text{O1}^i-\text{C14}^i$ DMA about the Ni—N3 axis.

is $\delta = 19^\circ$. This is not the case with the C12 and O2^* atoms; they are on opposite sides of the equatorial plane, and C12 approaches O2^* in the coplanar direction ($\delta = 74^\circ$).

The van der Waals closest contact distance is anisotropic for double-bonded oxygen (Bondi, 1964). The suggested value is significantly larger in the direction normal to the double bond (1.6–1.7 Å) than in the parallel direction (1.43 Å). Therefore, the steric repulsion between C22^* and O1^i may be beyond tolerance in the hypothetical conformation (Fig. 2b), leading to the twist of DMA, *i.e.* concerted rotation around the Ni— O2^* and $\text{O2}^*-\text{C21}^*$ bonds, to give rise to the actual conformation (Fig. 2a).

Experimental

The DMA solvate of $\text{Ni}(\text{BF}_4)_2$ was prepared as previously described (Suzuki & Ishiguro, 1992). The single crystal was

grown from a solution of the solvate in acetonitrile–diethyl ether mixture and sealed in a capillary tube in the glove box over P₂O₅.

Crystal data

[Ni(C₂H₃N)₂(C₄H₉NO)₄]-
(BF₄)₂
M_r = 662.93
Monoclinic
P2₁/c
a = 6.892 (3) Å
b = 19.706 (5) Å
c = 11.842 (2) Å
β = 94.24 (2)°
V = 1603.9 (9) Å³
Z = 2
D_x = 1.373 Mg m⁻³
D_m not measured

Mo Kα radiation
λ = 0.71073 Å
Cell parameters from 25 reflections
θ = 11–14°
μ = 0.686 mm⁻¹
T = 200 (2) K
Prism
0.40 × 0.30 × 0.30 mm
Green

Data collection

Enraf–Nonius CAD-4 diffractometer
ω–2θ scans
Absorption correction: ψ scan (North, Phillips & Mathews, 1968)
T_{min} = 0.627, T_{max} = 0.814
4880 measured reflections
4678 independent reflections

3256 reflections with I > 2σ(I)
R_{int} = 0.034
θ_{max} = 29.96°
h = -9 → 9
k = 0 → 27
l = 0 → 16
3 standard reflections
frequency: 60 min
intensity decay: 2%

Refinement

Refinement on F²
R[F² > 2σ(F²)] = 0.061
wR(F²) = 0.183
S = 1.152
4673 reflections
222 parameters
H atoms treated by a mixture of constrained and independent refinement

w = 1/[σ²(F_o²) + (0.0731P)² + 1.7845P]
where P = (F_o² + 2F_c²)/3
(Δ/σ)_{max} < 0.001
Δρ_{max} = 1.459 e Å⁻³
Δρ_{min} = -0.663 e Å⁻³
Extinction correction: none
Scattering factors from *International Tables for Crystallography* (Vol. C)

Table 1. Fractional atomic coordinates and equivalent isotropic displacement parameters (Å²)

$$U_{eq} = (1/3)\sum_i \sum_j U^{ij} a_i^* a_j^* \mathbf{a}_i \cdot \mathbf{a}_j$$

Ni	x	y	z	U _{eq}
O1	0.0730 (3)	-0.06638 (11)	0.1278 (2)	0.0322 (5)
O2	0.2141 (3)	-0.03382 (11)	-0.1021 (2)	0.0332 (5)
N1	0.1232 (5)	-0.15446 (15)	0.2438 (3)	0.0420 (7)
N2	0.2566 (5)	-0.0271 (2)	-0.2868 (3)	0.0464 (7)
N3	0.1910 (4)	0.06856 (14)	0.0822 (2)	0.0329 (6)
C11	0.1079 (4)	-0.1286 (2)	0.1401 (3)	0.0313 (6)
C12	0.1353 (6)	-0.1741 (2)	0.0414 (3)	0.0457 (8)
C13	0.1024 (7)	-0.1118 (2)	0.3429 (3)	0.0544 (10)
C14	0.1540 (9)	-0.2270 (2)	0.2662 (5)	0.074 (2)
C21	0.2869 (5)	-0.0040 (2)	-0.1824 (3)	0.0362 (6)
C22	0.4170 (6)	0.0571 (2)	-0.1617 (4)	0.0508 (9)
C23	0.1242 (7)	-0.0839 (2)	-0.3110 (4)	0.0570 (11)
C24	0.3462 (8)	0.0026 (3)	-0.3853 (4)	0.0679 (13)
C31	0.2904 (5)	0.1086 (2)	0.1219 (3)	0.0346 (7)
C32	0.4214 (7)	0.1600 (2)	0.1724 (4)	0.0588 (11)

B	0.6355 (8)	-0.3148 (3)	0.0187 (5)	0.0619 (13)
F1	0.4501 (6)	-0.3152 (3)	0.0448 (4)	0.144 (2)
F21†	0.671 (4)	-0.3149 (14)	-0.0884 (17)	0.154 (10)
F31†	0.772 (3)	-0.3443 (14)	0.0766 (11)	0.154 (10)
F41†	0.635 (3)	-0.2450 (5)	0.0552 (10)	0.112 (4)
F22‡	0.617 (3)	-0.3234 (10)	-0.0977 (13)	0.094 (5)
F32‡	0.672 (3)	-0.3802 (5)	0.0692 (10)	0.104 (4)
F42‡	0.755 (4)	-0.2723 (13)	0.0547 (14)	0.190 (11)

† Site occupancy = 0.49 (2). ‡ Site occupancy = 0.51 (2).

Table 2. Selected geometric parameters (Å, °)

Ni—O1	2.035 (2)	Ni—N3	2.078 (3)
Ni—O2	2.085 (2)		
O1—Ni—O2	94.54 (9)	O2—Ni—N3'	88.36 (10)
O1—Ni—O2'	85.46 (9)	Ni—O1—C11	138.5 (2)
O1—Ni—N3	87.49 (10)	Ni—O2—C21	129.1 (2)
O1—Ni—N3'	92.51 (10)	Ni—N3—C31	175.7 (3)
O2—Ni—N3	91.64 (10)		
Ni—O1—C11—N1	-169.9 (2)	Ni—O2—C21—N2	-113.4 (3)
Ni—O1—C11—C12	10.9 (5)	Ni—O2—C21—C22	69.0 (4)

Symmetry code: (i) -x, -y, -z.

Data were corrected for Lorentz, polarization and absorption effects. The structure was solved by direct methods and subsequent difference Fourier syntheses. Full-matrix least-squares refinement was performed. All non-H atoms were refined anisotropically. Methyl H atoms were placed at idealized positions with a fixed C—H distance and H—C—H angle, and refined using a rotating model *via* the *SHELXL93 HFIX 137* (Sheldrick, 1993) facility; the starting torsion angle was taken from the position of the maximum electron density in the loci of possible H-atom positions, and the displacement parameter was set as 1.5 times the equivalent isotropic displacement parameter of the methyl C atom. Disorder of three F atoms (F2–F4) was suggested by their highly anisotropic displacement parameters, so that two positions for each F atom were calculated by moving along the direction of the largest eigenvalue of the displacement tensor. A common site-occupation factor was assumed for three positions approximately tetrahedral with the non-disordered F1 atom. The occupation factors were refined under the constraint that the sum is three; the final values are 0.49 (2) for F21, F31 and F41, and 0.51 (2) for F22, F32 and F42. After the refinement, the displacement parameters for F31 were still somewhat anisotropic and the B—F distances show variation, but further attempts with more disordered positions did not converge. The maximum residual peak in the final difference Fourier map was near the Ni atom (0.75 Å apart).

Data collection: *CAD-4 Software* (Enraf–Nonius, 1989). Cell refinement: *CAD-4 Software*. Data reduction: *CAD-4 Software*. Program(s) used to solve structure: *SHELXS86* (Sheldrick, 1985). Program(s) used to refine structure: *SHELXL93*. Molecular graphics: *ORTEPIII* (Burnett & Johnson, 1996). Software used to prepare material for publication: *SHELXL93*.

This work has been financially supported by Grants-in-Aid for Scientific Research (No. 06453051) from the Ministry of Education, Science and Culture of Japan.

Supplementary data for this paper are available from the IUCr electronic archives (Reference: DE1060). Services for accessing these data are described at the back of the journal.

References

- Baumgartner, O. (1986). *Z. Kristallogr.* **174**, 253–263.
 Bondi, A. (1964). *J. Phys. Chem.* **68**, 441–451.
 Burnett, M. N. & Johnson, C. K. (1996). *ORTEP III. Thermal Ellipsoid Plot Program for Crystal Structure Illustrations*. Report ORNL-6895. Oak Ridge National Laboratory, Tennessee, USA.
 Enraf-Nonius (1989). *CAD-4 Software*. Version 5.0. Enraf-Nonius, Delft, The Netherlands.
 Herceg, M. & Fischer, J. (1974). *Acta Cryst.* **B30**, 1289–1293.
 Koide, M., Suzuki, H. & Ishiguro, S. (1995). *J. Chem. Soc. Faraday Trans.* **91**, 3851–3857.
 Lemoine, P. & Herpin, P. (1980). *Acta Cryst.* **B36**, 2772–2774.
 Lindner, E., Perdikatis, B. & Thasitis, A. (1973). *Z. Anorg. Allg. Chem.* **402**, 67–76.
 North, A. C. T., Phillips, D. C. & Mathews, F. S. (1968). *Acta Cryst.* **A24**, 351–359.
 Ozutsumi, K., Koide, M., Suzuki, H. & Ishiguro, S. (1993). *J. Phys. Chem.* **97**, 500–502.
 Sheldrick, G. M. (1985). *SHELXS86. Program for the Solution of Crystal Structures*. University of Göttingen, Germany.
 Sheldrick, G. M. (1993). *SHELXL93. Program for the Refinement of Crystal Structures*. University of Göttingen, Germany.
 Suzuki, H., Fukushima, N., Ishiguro, S., Masuda, H. & Ohtaki, H. (1991). *Acta Cryst.* **C47**, 1838–1842.
 Suzuki, H. & Ishiguro, S. (1992). *Inorg. Chem.* **31**, 4178–4183.
 Young, A. C. M., Walters, M. A. & Dewan, J. C. (1989). *Acta Cryst.* **C45**, 1733–1736.

Acta Cryst. (1997). **C53**, 1605–1606

Bis(η^5 -1,2,4-triisopropylcyclopentadienyl)-ruthenium

JASON S. OVERBY, JOHN M. FARRAR AND TIMOTHY P. HANUSA

Department of Chemistry, Vanderbilt University, Nashville, TN 37235, USA. E-mail: hanusat@ctrvax.vanderbilt.edu

(Received 25 September 1996; accepted 12 May 1997)

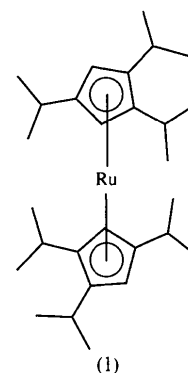
Abstract

The title compound, $[\text{Ru}\{(\text{C}_3\text{H}_7)_3\text{C}_5\text{H}_2\}_2]$, displays a rigorously parallel sandwich geometry, with the Ru atom residing on a crystallographically imposed inversion center. A resolvable disorder is present in one isopropyl substituent. The average Ru—C(ring) distance is 2.182(9) Å, similar to that of other structurally characterized ruthenocenes.

Comment

We have been examining the effects of bulky isopropylated cyclopentadienyl rings on the structural, electrochemical and magnetic properties of first-row transition metal metallocenes (Burkey, Hays, Duderstadt & Hanusa, 1997). As an extension of this research to larger second-row transition metals, we have prepared

the ruthenocene $[(\text{C}_3\text{H}_7)_3\text{C}_5\text{H}_2]_2\text{Ru}$, (1), and determined its crystal structure.



The structure of (1) contains a crystallographically imposed inversion center at the Ru atom. Consequently, the cyclopentadienyl rings are rigorously parallel, making (1) isostructural with $[(\text{C}_3\text{H}_7)_3\text{C}_5\text{H}_2]_2M$ ($M = \text{Fe}, \text{Co}$; Burkey *et al.*, 1997). The average Ru—C bond length is 2.182(9) Å, with individual bond lengths ranging from 2.168(4) to 2.191(4) Å. Despite the steric bulk of the rings, the average Ru—C bond length in (1) is comparable with that in $(\text{C}_5\text{H}_5)_2\text{Ru}$ (average 2.191 Å; Seiler & Dunitz, 1980) and $(\text{C}_5\text{Me}_5)_2\text{Ru}$ [average 2.17(1) Å; Albers *et al.*, 1986], but is less than that in the more sterically encumbered $[(\text{C}_6\text{H}_5)_4\text{C}_5\text{H}_2]_2\text{Ru}$ (average 2.202 Å; Hoobler *et al.*, 1991). The range of Ru—C bond distances in (1) ($\Delta = 0.023$ Å) is intermediate between $(\text{C}_5\text{H}_5)_2\text{Ru}$ (range 2.181–2.188 Å, $\Delta = 0.007$ Å) and $[(\text{C}_6\text{H}_5)_4\text{C}_5\text{H}_2]_2\text{Ru}$ (range 2.181–2.214 Å, $\Delta = 0.033$ Å), an illustration of the progressively greater steric effect of the triisopropyl- and tetraphenylcyclopentadienyl rings. There is only a slight displacement of the methine C atoms of the isopropyl substituents in (1) from the cyclopentadienyl ring plane (average 0.11 Å); this amount is similar to that in $[(\text{C}_3\text{H}_7)_3\text{C}_5\text{H}_2]_2\text{Fe}$ (0.12 Å) and slightly less than in $[(\text{C}_6\text{H}_5)_4\text{C}_5\text{H}_2]_2\text{Ru}$ (0.14 Å).

A distinctive feature of (1) not found in analogous first-row metallocenes is the resolvable disorder in the isopropyl substituent on C(2). Assignment of occupancy factors 0.60 and 0.40 to C(8), C(9) and C(8A), C(9A), respectively, led to satisfactory refinement of the methyl C atoms. In the iron and cobalt structures, this isopropyl group displays larger displacement parameters than the other two, but the relatively close interring distances and long intermolecular contacts [*i.e.* 3.32 and 3.84(1) Å, respectively, in $[(\text{C}_3\text{H}_7)_3\text{C}_5\text{H}_2]_2\text{Fe}$] probably prevents any observable disorder. In (1), the interplanar distance (3.63 Å) is comparable with the closest intermolecular contact [3.62(1) Å between C(8) and C(11)(*x*, *-y*, *z*)]. The greater freedom for rotation combined with the close packing evidently encourages the C(2) isopropyl group in (1) to adopt more than one conformation.